Heliyon 11 (2025) e42014

Contents lists available at ScienceDirect

Heliyon

journal homepage: www.cell.com/heliyon

Research article

Computational design, expression, and characterization of a *Plasmodium falciparum* multi-epitope, multi-stage vaccine candidate (PfCTMAG)

Joan A. Chick [a], Nadege N. Abongdia [a], Robert A. Shey [b], Tobias O. Apinjoh [a,b,*]

[a] *Department of Chemical and Biological Engineering, National Higher Polytechnic Institute, The University of Bamenda, Cameroon*
[b] *Department of Biochemistry and Molecular Biology, Faculty of Science, University of Buea, Cameroon*

ARTICLE INFO

Keywords:
In silico
Vaccine candidate
Sero-reactivity
Multi-epitope
Immunogenicity

ABSTRACT

Malaria, a tropical disease, claims the lives of thousands of people annually and the development of resistance to insecticides and antimalarial drugs poses a great challenge to current prevention and control strategies. Current malaria vaccines are limited in efficacy, duration of protection, and safety, due to the high antigenic diversity and complex life cycle of the *Plasmodium* parasite. This study sought to design and assess a more effective multi-stage, multi-epitope vaccine candidate for the control of malaria. A multi-epitope malaria vaccine candidate was designed *in silico* using multiple antigens from both the pre-erythrocytic and erythrocytic stages, expressed in bacteria, and its sero-reactivity to antibodies in plasma from malaria-positive (cases) and negative individuals (controls) was assessed using enzyme-linked immunosorbent assay (ELISA). Immunization experiments were equally conducted with BALB/c mice. *In-silico* analysis revealed that the designed antigen, PfCTMAG (*Plasmodium falciparum* Circumsporozoite, Thrombospondin-related adhesion protein, Merozoite surface protein 2, Apical asparagine (Asn)-rich protein and Glutamate-Rich Protein), effectively bound to Toll-like receptor 4 (TLR-4) and triggered a strong immune response. In sero-reactivity studies, malaria-positives (cases) had higher anti-PfCTMAG IgG ($\boldsymbol{p = 0.024}$) and IgM ($\boldsymbol{p < 0.001}$) levels compared to malaria negatives (controls). The mice immunized with PfCTMAG did not show adverse reactions and had higher levels of IgG antibodies ($p = \mathbf{0.002}$) compared to controls, thereby validating the safety and immunogenicity of PfCTMAG as a promising vaccine candidate.

Abbreviations: APC, Antigen Presenting Cell; COVID-19, Corona Virus Disease of 2019; CTL, Cytotoxic T lymphocyte; ELISA, Enzyme-linked Immunosorbent Assay; EDTA, Ethylenediaminetetraacetic Acid; GRAVY, Grand Average Hydropathicity; HTL, Helper T lymphocyte; HRP, Horse-Radish Peroxidase; IDRs, Intrinsic Disordered Regions; IEDB, Immune epitope database; IgG/IgM, Immunoglobulin G/M; IL4/10, Interleukin 4/10; ITNs, Insecticide-Treated Nets; IRS, Indoor Residual Spray; LBL, Linear B-lymphocyte; LC-MS, Liquid Chromatography-Mass Spectrometry; MEV, Multi-Epitope Vaccine; MHC, Major Histocompatibility Complex; mRDT, malaria Rapid Diagnostic Test; NMA, Normal Modes Analyses; OD, Optical Density; PFCTMAG, *Plasmodium falciparum* Circumsporozoite, Thrombospondin-related adhesion protein, Merozoite surface protein 2, Apical asparagine (Asn)-rich protein and Glutamate-Rich Protein; RMSD, Root Mean Square Deviation; SDS-PAGE, Sodium Dodecyl Sulfate-Polyacrylamide Gel Electrophoresis; SVM, Support Vector Machine; TLR-4, Toll-Like Receptor 4; TMB, 3,3′,5,5′-Tetramethylbenzidine.

* Corresponding author. Department of Chemical and Biological Engineering, National Higher Polytechnic Institute, The University of Bamenda, Cameroon.

E-mail address: apinjoh.tobias@ubuea.cm (T.O. Apinjoh).

https://doi.org/10.1016/j.heliyon.2025.e42014
Received 25 September 2024; Received in revised form 13 January 2025; Accepted 15 January 2025
Available online 18 January 2025

1. Introduction

Malaria remains a serious global health concern, causing significant morbidity and mortality especially in children under the age of five, pregnant women, and people with weakened immune systems in Africa [1]. Various strategies have been implemented to combat the disease including the use of antimalarial drugs, insecticide-treated bed nets (ITNs), and indoor residual sprays (IRS). However, the effectiveness of these tools is being jeopardized by the widespread resistance of the mosquito vector and parasite to insecticides and antimalarial drugs (including Artemisinin-based combination therapies) respectively [2]. There is, therefore, the need to develop more effective strategies to control and ultimately eliminate the parasite.

Vaccines have demonstrated remarkable efficacy in preventing numerous infectious diseases but the development of vaccines against the malaria parasite has been limited by the complexity of the parasite's biology, its ability to evade immune responses, and the intricacy of the parasite's infection cycle [3,4]. Malaria vaccine candidates can be classified as pre-erythrocytic, erythrocytic, or transmission-blocking depending on the specific stage of the life cycle they target [5]. The first approved malaria vaccine, RTS, S/AS01 [6] demonstrated only a 36 % reduction in clinical malaria episodes in Phase III trials among African children. Additionally, neonates required up to four doses of the vaccine to experience only a 26 % reduction in severe malaria [7]. R21/MATRIX-M, the second approved vaccine has shown a remarkable ability to decrease symptomatic cases of malaria by 75 % but equally requires multiple doses [8]. Additionally, both vaccines only provide protection against the pre-erythrocytic stage of the life cycle but not the blood stage. A multi-stage vaccine that can confer protection against more than one life cycle stage will likely have a better efficacy [5].

Conventional vaccines, made up of weakened or inactivated forms of an infectious agent often have limited efficacy and safety concerns attributed to inadequate exposure of the antigen to the immune system, poor antigenic response, and allergenicity to the host [9]. However, advancements in reverse vaccinology have allowed the prediction of molecule(s) with the necessary qualities of a suitable vaccine candidate [10]. In recent years, reverse vaccinology coupled with immuno-informatics has revolutionized vaccine development, leveraging vast databases and tools to design safer and more efficacious multi-epitope vaccines [11,12]. This innovative approach has demonstrated its effectiveness in designing vaccines for COVID-19 [13,14] as well as malaria [15]. However, vaccines designed computationally need to be validated using wet lab experiments. As such, this study employed *in silico, in vitro,* and *in vivo* methods to design and characterize a vaccine candidate against *P. falciparum*. The multi-stage multi-epitope vaccine candidate, PfCTMAG was designed *in silico* using the **C**ircumsporozoite protein (CSP), **T**hrombospondin-Related Adhesion Protein (TRAP), **M**erozoite Surface Protein 2 (MSP2), **A**pical Asparagine (Asn)-Rich Protein (AARP), and **G**lutamate-Rich Protein (GLURP). The level of circulating antibodies against PfCTMAG was then quantified *in vitro* in malaria-infected human plasma samples by ELISA, followed by safety and immunogenicity assessment, *in vivo* through mice immunization.

2. Materials and methods

2.1. Ethical considerations

Ethical clearance was obtained from the Institutional Review Board of the Faculty of Health Sciences of the University of Bamenda (2023/0869H/UBa/IRB) on March 29, 2023, while administrative authorization was obtained from the South West Regional Delegation of Public Health. The clearance for animal studies was obtained from the University of Buea Institutional Animal Care and Use Committee (UB-IACUC No 20/2023) on September 20, 2023.

2.2. Study design

The study comprised an *in-silico* design, subsequent sample collection through a cross-sectional case-control, and a cohort study from July to August 2023 during the rainy season.

2.3. Study participants

Given that malaria immunity is age-dependent with a weaker immune response in children, stronger response in adults, and declining response in the elderly, we selected participants [16] between the ages of 18–65 years for enrollment. Cases included microscopy and mRDT (malaria rapid diagnostic test) positive individuals reporting to selected health facilities while controls consisted of age- and gender-matched blood film and mRDT negative participants from health facilities, blood donors as well as apparently healthy individuals (individuals with no observed symptoms of disease) from the community. A pool of 5 malaria-naïve European sera was used as the negative control for the assay.

2.4. Study area

This research was conducted in Buea (4° 10′0″N 9°14′0″E) which is found in the Fako Division, South West Region of Cameroon. Buea has an equatorial climate with average temperatures ranging between 20 and 33 °C daily, high humidity, and rainfall (2625 mm annually). Buea has 2 distinct seasons: a long rainy (March–November) and short dry (November-March) [17]. Malaria prevalence in the study area exhibits seasonal variation, meso-endemic (moderate transmission) during the dry season but becomes hyper-endemic (intense transmission) during the rainy season. *Plasmodium falciparum*, transmitted primarily by the *Anopheles gambiae* mosquito, is responsible for up to 96 % of malaria cases in this region [18]. Blood samples were collected at the main government (Regional

Hospital Buea) and private (Solidarity Health Foundation) hospitals in the area, as well as the surrounding community (Molyko) from June to August 2023. After collection, samples were transported to the Parasitology Laboratory at the Faculty of Health Sciences, University of Buea for storage and analysis.

2.5. Sample size

From a similar study by Nebie et al., we used the same effect size of 0.18 [19], $\alpha = 0.05$, power = 0.8, and a two-tailed test in the G*Power software, *A priori* sample size of 123 participants per group was obtained. Allowing for 10 % missingness, a minimum of 135 samples per group was required to conduct the case-control study. The number of mice (N) was determined using the resource formula N = (DF/k)+1 at (LINK) where k refers to the number of groups and $10 \leq DF \leq 20$ [20]. Given the estimated minimum of 5 mice and a maximum of 7 mice per group, 6 mice per group were enrolled for the 3 groups in this study.

2.6. Construct design

2.6.1. Retrieval of protein sequences

Fourteen previously reported pre-erythrocytic and erythrocytic *P. falciparum* vaccine candidates: Circumsporozoite protein (CSP), Cell-traversal protein for ookinetes and sporozoites (CelTOS), Thrombospondin-related adhesion protein (TRAP), Liver-stage antigen 3 (LSA3), *P. falciparum* schizont egress antigen 1 (PfSEA-1), Serine repeat antigen 5 (SERA5), Merozoite surface protein 1 (MSP1), Merozoite surface protein 2 (MSP2), Merozoite surface protein 3 (MSP3), Apical membrane antigen 1 (AMA-1), Erythrocyte binding antigen 175 (EBA175), Glutamate-Rich Protein (GLURP), Reticulocyte binding homolog (RH5), and Apical asparagine (Asn)-rich protein (AARP) were selected following literature review. Their sequences were retrieved from PlasmoDB and antigenicity was predicted using Vaxijen v2.0 (LINK). Based on their antigenicity scores, two pre-erythrocytic (CSP and TRAP), two erythrocytic (MSP2 and AARP) specific, and GLURP which belong to both stages were retained for further analyses. For each step of the *in-silico* design, we selected the most commonly used tools from the literature, and in most cases we used more than one tool to account for the differences in their algorithms.

2.6.2. Prediction of subcellular localization

DeepLoc v2.0 and WoLFpSORT were used to predict where the selected antigens reside within the cell. DeepLoc v2.0 (LINK) uses solely the sequence information for prediction [21] while WoLFpSORT (LINK) predicts by converting amino acid sequences to features like sorting signals and functional motifs [22].

2.6.3. Prediction of signal peptide and transmembrane domains

SignalP6.0 and PrediSi were used to predict the presence of signal peptides. SignalP6.0 (LINK) excels at discriminating classical secretory from non-secretory proteins [23]. PrediSi (LINK) offers versatility, predicting cleavage sites and signal peptide presence [24]. TMHMM v2.0 and TOPCONS were used to predict the presence of transmembrane helices. The TMHMM v2.0 server (LINK) is based on a hidden Markov model and effectively differentiates soluble from membrane proteins [25]. TOPCONS (LINK) provides a consensus prediction of membrane protein topology [26]. Following the prediction process, all identified signal peptides and transmembrane helices were cleaved.

2.6.4. Selection of Linear B-lymphocyte (LBL) epitopes

The BepiPred v2.0 and SVMTrip servers were used to predict LBL epitopes. The BepiPred v2.0 server (LINK) leverages a novel algorithm to predict LBL epitopes. This method, trained on known 3D structures of antibody-antigen complexes and a vast database of epitopes from the immune epitope database (IEDB), utilizes a random forest algorithm and has superior performance compared to other tools [27]. On the other hand, SVMTriP (LINK) employs a support vector machine (SVM) approach for prediction and incorporates a scoring system based on tri-peptide similarity and propensity to enhance the accuracy of its predictions [28]. From BepiPred v2.0, we only selected epitopes above the threshold of 0.5 and with lengths between 12 and 20, and from SVMTrip we selected epitopes with a score of 1.000.

2.6.5. Selection of T cell epitopes

This is aimed at pinpointing short sequences in an antigen with the ability to trigger immune responses mediated by $CD4^+$ or $CD8^+$ T cells [29]. NetCTL 1.2 (LINK) predicts MHCI binding peptides and was therefore used to predict cytotoxic T lymphocytes (CTL) epitopes for MHC supertypes A2, A3, and B7, with a 0.75 threshold, a C-terminal cleavage weight of 0.15, and a TAP efficiency weight of 0.05 [30]. We selected only CTL epitopes with scores greater than 0.75. Prediction of Helper T cell (HTL) epitopes was performed using the NetMHCII 2.3 server (LINK). NetMHCII 2.3 is an allele-specific approach and predicts peptide binding to human leukocyte antigens (HLA) and mouse H2 alleles. The program also identifies both strong and weak binding peptides [31]. The cutoff for binding affinity values was set at < 50 nm, and we only selected HTL epitopes that were strong binders.

2.6.6. Evaluation of epitopes

The antigenicity prediction for all LBL, CTL, and HTL epitopes was performed using VaxiJen v2.0 and ANTIGENpro servers. VaxiJen v2.0 (LINK) employs an alignment-independent, predicting antigenicity with an accuracy rate of approximately 88 %. The threshold for antigenicity prediction varies depending on the target organism selected on this server [32]. ANTIGENpro (LINK) uses an

SVM classifier to analyze the results from various protein sequence analyses and ultimately predicts whether the protein is antigenic along with a probability score [33]. The allergenicity of the epitopes was predicted using the AllergenFP v1.0 and AllerTOP v2.0 servers. AllergenFP v1.0 (LINK) utilizes an alignment-free approach, analyzing the protein sequence itself based on various physicochemical properties. It has been reported to be accurate in identifying allergens, achieving 88 % [34]. Meanwhile, AllerTOP v2.0 (LINK) is based on amino acid E-descriptors, auto and cross-variance transformation, and machine learning methods such as k-nearest neighbours [KNN] algorithm with an 85.3 % prediction accuracy [35]. Prediction of epitope toxicity status was done using ToxinPred (LINK) [36]. Therefore, only epitopes with antigenicity scores greater than 0.5, nonallergic and nontoxic were selected for further analysis.

2.6.7. Conservation of epitopes

To determine the potential of cross-protection to related *Plasmodium* species (*P. vivax, P. knowlesi, P. malariae, and P. ovale)*, a BLAST was done for each selected antigen. BLASTp (LINK) identifies regions of similarity between protein sequences [37]. For each antigen, the homolog with the greatest percentage identity per *Plasmodium* specie was selected. The IEDB Epitope Conservancy Analysis tool LINK was used to predict the level of conservation of the epitopes across these four species of *Plasmodium* [38].

2.6.8. Multi-epitope vaccine construction

In order to avoid the expression complexities often associated with large proteins, we aimed to keep the designed protein short and easy to express. We ranked the selected epitopes for each class (LBL, CTL, HTL) by their antigenicity scores and to keep a balance between the classes, we selected the six (6) top-ranking epitopes from each class making a total of 18 epitopes used in designing the vaccine candidate. A synthetic TLR-4 agonist, RS09 (APPHALS) was added at the N-terminal as an adjuvant [39]. The first top LBL epitope was combined with the adjuvant using an EAAAK linker, while the remaining LBL epitopes were joined using the KK linker. The AAY linker was used to connect the CTL epitopes and the GPGPG linker was employed to join the HTL epitopes together. Finally, a 6x His-tag was added at the C-terminal.

2.6.9. Analysis of physicochemical properties and solubility

The construct's physicochemical properties were evaluated using ExPASy-ProtParam (LINK), an online tool that predicts properties like molecular weight, grand average hydropathicity (GRAVY) value, theoretical isoelectric point (pI), instability index (II), half-life, and aliphatic index [40]. For the assessment of solubility upon expression in *E. coli*, SOLpro at (LINK) with an estimated overall accuracy of over 74 % was applied [41]. Furthermore, allergenicity prediction (using AllerTOPv 1.0 and AllegenFP v2.0) and antigenicity prediction (using Vaxijen and ANTIGENpro) for the construct was performed.

2.6.10. Prediction of cytokine responses

The presence of IFN-γ epitopes was predicted by scanning the designed construct on the IFNepitope server (LINK). This server is specifically designed to identify peptides from protein sequences that have the potential to induce IFN-γ release from $CD4^+$ T cells [42]. Next, IL-4 and IL-10 inducers were identified with the IL4pred (LINK) [43] and IL10pred servers (LINK) [44] respectively.

2.6.11. Prediction of secondary structure and disordered regions

PSIPRED and SOPMA were employed for secondary structure prediction of the vaccine construct. PSIPRED (LINK) employs a position-specific technique to find similar sequences and predicts alpha-helices, beta-sheets, coil structures, and other features with an accuracy of around 84.2 % [45]. The SOPMA server (LINK) is another server that was used to predict secondary structure features in the designed candidate [46]. For this study, the default parameters of the SOPMA tool were maintained.

2.6.12. Prediction of intrinsic disordered regions (IDRs)

These regions have been established as structural antigens [47] with numerous vaccine candidates in *Plasmodium* containing significant disordered regions [48]. For PfCTMAG, IDRs were predicted using IUPred3 (LINK). IUPred3 is capable of identifying protein regions that either form a stable structure or remain disordered based on the redox conditions of their environment [49].

2.6.13. Tertiary structure prediction, refinement, and validation

The sequence of the designed construct was submitted to the I-TASSER server (LINK) which is a top-ranked platform for automated protein structure and function prediction from amino acid sequences. It achieves this by analyzing multiple threading alignments and performing iterative simulations [50]. The resulting 3D models were visualized using a software called PyMOL (LINK). To further refine the 3D structure and improve its quality, a two-step process with ModRefiner and GalaxyRefine was employed. ModRefiner (LINK) first tackled the core structure (Cα traces) through energy minimization, leading to better overall and local structures with more accurate side-chain positions and fewer clashes between atoms [51]. GalaxyRefine (LINK) then focused on reconstructing the side chains, generating five refined models in total [52]. To assess the overall quality of the 3D model, a score (Z-score) was calculated by ProSA-web (LINK) [53]. Additionally, ERRAT SAVES v6.0 (LINK) was used to predict high-resolution crystallography structures to evaluate interactions between atoms [54]. Finally, the Ramachandran plot generated by PROCHECK (LINK) served as a final validation step. This plot visualizes the allowed angles for amino acid backbones (psi [ψ] and phi [ϕ] angles), ensuring the structure adheres to biophysical constraints [55].

2.6.14. Prediction of discontinuous B-cell epitopes

To identify potential discontinuous B-cell epitopes within the vaccine construct, ElliPro (LINK), a cutting-edge tool that treats the protein as an ellipsoid was utilized. It is a structure-based method known for its superior performance in epitope prediction [56].

2.6.15. Molecular docking with TLR-4, MHC-I, and MHC-II

To assess how the vaccine construct might interact with immune system receptors, PatchDock (LINK), which performs structure prediction of protein-protein and protein-small molecule complexes was used for docking assessment of the refined 3D structure with human TLR-4 (PDB ID: 5IJB), MHC-I (PDB ID: 1I1Y), and MHC-II (PDB ID: 1KG0) receptors from RCSB PDB [57]. Refinement and re-scoring of the top 10 models was performed with FireDock (LINK), which ranked them by their global energy [58].

2.6.16. Molecular dynamics simulation

To understand the flexibility and movements of the docked vaccine-receptor complex, iMODS (LINK) which analyzes normal modes (NMA) of the complex, predicting its deformability, characteristic motions, and stability based on factors like eigenvalues and B-factors [59] was used.

2.6.17. Immune simulation analysis

To predict the immune response to the vaccine candidate, the C-ImmSim server (LINK), a program that combines immune epitope prediction and machine learning to assess immune interactions, was used [60]. For the simulation of the vaccine construct responses, three doses were injected with a time step of 14 days between doses.

2.6.18. Codon optimization and in-silico cloning

To predict its expression conditions within the *E. coli* strain K12 prokaryotic expression system, reverse translation of the amino acid sequence to DNA and codons optimized using the Java Codon Adaptation Tool (JCAT) (LINK) [61], which further predicted the codon adaptation index (CAI) and GC content [62]. Finally, a plasmid map was designed using SnapGene for integration into a pET-30a (+) expression vector.

2.6.19. Protein expression and purification

The DNA sequence of PfCTMAG was sent to GenScript (Netherlands) for optimization, synthesis, and cloning into a pET-30a (+) vector. The resulting plasmid was transformed into competent *E. coli* strain BL21 Star™ (DE3) cells and a single colony was selected for inoculation into LB medium supplemented with kanamycin. The culture was incubated at 37 °C until the optical density (OD600) reached 1.2. Protein production was then induced with IPTG at 37 °C for 4 h. Cells were harvested by centrifugation, and the cell pellets were re-suspended in lysis buffer followed by sonication to break down the cells. The lysate was centrifuged again to separate soluble and insoluble components. The protein of interest was then extracted from the precipitate using guanidine hydrochloride, and subsequently purified using a nickel affinity column. The concentration was determined by Bradford protein assay. Purity was determined using standard SDS-PAGE and confirmed with Western blot and LC-MS.

2.7. Assessment of seroreactivity in cases and controls

2.7.1. Sample collection and processing

Information on socio-demographic and clinical parameters was recorded using a structured questionnaire. Two (2) mL of venous blood were collected from each selected participant and transferred into tubes containing EDTA (BD Vacutainer Systems, Plymouth, UK). Following malaria parasitaemia and Hb determination, plasma was separated from packed cells by centrifugation at 3000×*g* for 10mins and the plasma aliquoted into 1.5 mL Eppendorf tubes and stored at −86 °C for antibody measurement.

2.7.2. Haemoglobin measurement

Haemoglobin levels were measured using a hemoglobinometer (Hangzhou Sejoy Electronics, China) according to the manufacturer's instructions. Anemic status was defined as Hb < 11.0 g/dL [63].

2.7.3. Malaria diagnosis

The presence of *P. falciparum* was diagnosed via two methods. First, a rapid diagnostic test (RDT) using the PfHRP2/pLDH malaria kit (AdvDx™ Malaria Pf test) was performed following the manufacturer's instructions. Briefly, 5 μL of blood were added to the sample well, followed by three drops of diluent and allowed to run for 15 min. The presence of two (test and control), one (control only), and no (or one at the test) line(s) indicated a positive, negative or an invalid test result respectively. Secondly, microscopic examination was conducted following WHO guidelines. Thick and thin blood smears were prepared on microscope slides, stained with 10 % Giemsa for 10 min, and examined for the presence of *P. falciparum* under oil immersion with the 100x objective, 10× eyepiece of a binocular light microscope (Olympus Optical Co., Ltd, Japan) [64]. Parasitaemia was determined in the thick film by counting the number of parasites relative to at least 200 white blood cells, assuming an average white blood cell count of 8000 per microliter [65] while thin films were used for *Plasmodium* species identification. Two independent microscopists reviewed the slides, with a third reading performed for discrepancies. If no malaria parasites were seen in 100 high-power fields, then the smear was declared negative.

Therefore,

$$\text{Parasites} \Big/ \mu\text{L blood} = \frac{\textit{Number of parasites counted x 8000 white bloodcells}/\mu L}{\textit{No. of white blood cells counted}}$$

2.7.4. Measurement of IgG and malaria diagnosis

All plasma samples were tested for the presence of *P. falciparum*-specific IgG and IgM antibodies against the expressed antigen using ELISA. Prior to the assay, the optimal concentrations were determined through checkerboard titrations were 2.5 μg/mL for antigen and 1:250 plasma dilution for both IgG and IgM. Microtiter plates (Costar, Cambridge, MA) were coated with the antigen in 0.1M, pH 9.6 carbonate buffer (100 μL/well) overnight at 4 °C and blocked for 2 h at 37 °C with 200 μL Phosphate Buffered Saline – Tween 20 (PBST) containing 0.5 % non-fat milk to prevent non-specific binding. Plasma samples diluted to the optimal concentration were added to duplicate wells, incubated for 1 h at 37 °C with 100 μL diluted plasma/well, and washed with PBST. Goat anti-human IgM or IgG Fc-HRP (Southern Biotech, USA) were added to probe for bound antibodies. After incubation with the HRP conjugates, TMB (Glentham Life Sciences Ltd) was added as substrate, and the enzymatic reaction stopped with 100ul of 1M sulfuric acid. The intensity of the color change was read at 450 nm using an ELISA plate reader (SINOTECH, Shanghai, China). A positive result (seropositivity) was defined as samples with ODs exceeding the mean OD for the 5 non-immune European donors + 2 standard deviations (SD).

2.8. Safety and immunogenicity in animal model

Given that BALB/c mice tend to produce a stronger humoral immune response compared to most common mouse strains [66], a total of eighteen (18) BALB/c mice aged between 8 and 12 weeks were purchased and kept at the animal house of the University of Buea. The mice were randomly divided into 3 groups (Prime, Booster, and Control) containing 3 males and 3 females each and allowed to acclimatize for 5 days before the experiments. On day 0, the Prime and Booster groups were immunized intramuscularly with 50 μg antigen in 100 μl PBS while mice in the control group received 100 μL of 1x PBS. On day 14, only the mice in the Booster group were administered a second (booster) dose of same concentration. All mice were observed daily and their weights were recorded on days 0, 3, and 7. Blood was collected via facial bleeding from each mouse on days 0 (baseline for immune response measurement), 14 (usually where peak primary immune responses occur for most vaccines), and 28 (to assess the sustained primary immune response or the secondary response from a booster dose) [67]. The blood was centrifuged at 4 °C, and the plasma samples were aliquoted and stored at −20 °C until use in ELISA. All mice were euthanized on day 28 by injecting with an anesthetic followed by decapitation.

The ELISA procedure was conducted as described in 2.2.4 above but the human plasma was replaced with mice plasma and probed with goat anti-mouse IgG Fc-HRP and IgM-HRP. Seropositivity was defined as test samples with an OD greater than the mean + 2 SD of the ODs recorded on day 0 of each group before immunization.

2.9. Data analysis

Data analysis was done with the SPSS statistics version 29 (IBM® Chicago, USA). Comparisons between the means of two groups (cases and controls) were done using the student's t-test and the Kruskal-Wallis H was used for the three different groups of mice with the Bonferroni correction to reduce the likelihood of false positives for pairwise comparisons. To compare proportions between groups, the Pearson χ^2 test was used. A $p\text{-value} < 0.05$ was considered significant.

3. Results

3.1. Construct design

3.1.1. Antigenicity, localization, signal peptides and TMHs of antigens

The predicted antigenicity scores of the selected proteins were ranked in order of decreasing antigenicity per stage (Supplementary materials Table S1). For the pre-erythrocytic stage, CSP had the highest antigenicity score followed by TRAP, for the erythrocytic stage, MSP2 and AARP had the highest scores while for antigens found in both stages, GLURP had a higher score. The chosen antigens were predicted by one or both servers to be present in the cell membrane or extracellular matrix implying they are exposed to the host immune system and are likely to be good targets for vaccine development. Signal peptides and transmembrane helices (TMHs) were each predicted in 3 of the 5 antigens (Supplementary materials Table S2). The signal peptide sequences and TMHs of CSP, TRAP, and GLURP were cleaved prior to further analysis while the entire amino acid sequence of MSP2 and AARP were retained.

3.1.2. Epitope prediction and selection

After stages of screening based on antigenicity, allergenicity and toxicity scores, we selected only epitopes that were nonallergic, nontoxic with antigenicity score greater than the 0.5 threshold for parasites. To keep the ratio of LBL, CTL and HTL equal, we selected the same number of epitopes for each and since HTL only had 6 epitopes that met our selection criteria, we also selected 6 from LBL and 6 from CTL. The final epitopes for the construction therefore included 18 top-scoring LBL, CTL, as well as high-binding HTL epitopes (Supplementary materials Table S3).

3.1.3. Conservation of epitopes

A BLAST query of the chosen proteins revealed that they were conserved in the selected human malaria-causing *Plasmodium* species

(*P. vivax, P. knowlesi, P. malariae and P. ovale*) and share no homology with *Homo sapiens*. The homologues with the greatest conservancy for each species was chosen for epitope conservancy analysis on IEDB. All epitopes were conserved to some extent in the chosen homologues with a minimum and maximum identity of 22.73 % and 90 % respectively (Supplementary materials Table S4).

3.1.4. Vaccine construction

The sequence of PfCTMAG was 354 amino acids long starting with the adjuvant sequence at the N-terminal to enhance immunogenicity, followed by the different epitope sequences joined by their respective linkers, and lastly a C-terminal 6x His-tag to aid in purification (Fig. 1).

3.1.5. Prediction of antigenicity, allergenicity, and toxigenicity

Vaxijen2.0 predicted the protein's antigenicity to be 1.2049 (threshold = 0.5 for parasites) while ANTIGENpro predicted a 0.551496 probability of antigenicity. AllerTOP v2.0 and AllergenFP v1.0 predicted the protein to be non-allergenic while ToxinPred predicted the protein to be non-toxic.

3.1.6. Physicochemical features of the chimeric vaccine construct

PfCTMAG had a predicted theoretical pI of 10.03 indicating a basic nature, a low molecular weight of 37431.57 (~37 kDa), an instability index of 28.27 which is less than 40, indicating it's stable, an aliphatic index of 45.28, a favourable half-life of 30 h *in vitro* in mammalian reticulocytes and 10 h *in vivo* in *E. coli*. The Grand average of hydropathicity (GRAVY) was −1.279 with the negative indicating a hydrophilic nature and the predicted solubility score of 0.922015 validating its solubility when expressed in *E. coli*.

3.1.7. IFN-γ-inducing epitopes

Three hundred and forty-six (346) potential IFN-γ-inducing epitopes (overlapping 15-mer sequences) of which 158 had a positive score between 0 and 2 were predicted for the protein. The construct was predicted to contain a total of 211 IL-4-inducing epitopes with positive Support Vector Machine (SVM) scores ranging from 0.2 to 1.01 and 340 IL-10-inducing epitopes with scores from 0.31 to 0.66. This suggests that PfCTMAG has the potential to trigger a strong cytokine response.

3.1.8. Prediction of IDRs

The protein was predicted to be mostly composed of disordered regions as a majority of the residues were found above the threshold of 0.5 (Fig. 2). These disordered regions are advantageous to vaccine candidates since they do not have a fixed structural conformation and hence are flexible in their binding with products of the immune system.

3.1.9. Secondary structure prediction

The PfCTMAG antigen was predicted to be comprised of 11.30 % (40) alpha helix, 13.56 % (48) extended strand, 5.37 % (19) beta turn and 69.77 % (247) random coil by SOPMA. The PSIPRED tool predicted the protein to be mostly composed of coils, followed by helix and strands (Fig. 3).

3.1.10. Tertiary structure modeling, refinement and validation

I-TASSER used ten best templates (7t3uA, 3jc8Q, 6f2r, 2c3fA, 7wahA, 5fmwA, 7s7bB, 2nbiA, 7ptpA, 4n16A) to predict five models with C-scores ranging between −5 and 2 with more positive values reflecting a higher quality. Model 1 with the greatest C-score of −1.75, TM-Score of 0.50 ± 0.15, and RMSD of 10.6 ± 4.6A° was selected. Model 1 was initially refined using ModRefiner (RMSD = 0.960, TM-score = 0.9819) followed by another round of refinement using GalaxyRefine which yielded five models and the refined model with the greatest GDT-HA (0.9456) and the lowest MolProbity (2.242) was chosen (Fig. 6A). The ERRAT value of the construct was 81.3291 which indicates the model is of good quality, supported by a Z-score of −4.05 which was within the range of native proteins of similar structure. The Ramachandran plot indicated 84.8 % favoured, 11.6 % additionally allowed, 1.8 % generously allowed and 1.8 % disallowed regions (Supplementary materials Fig. S1).

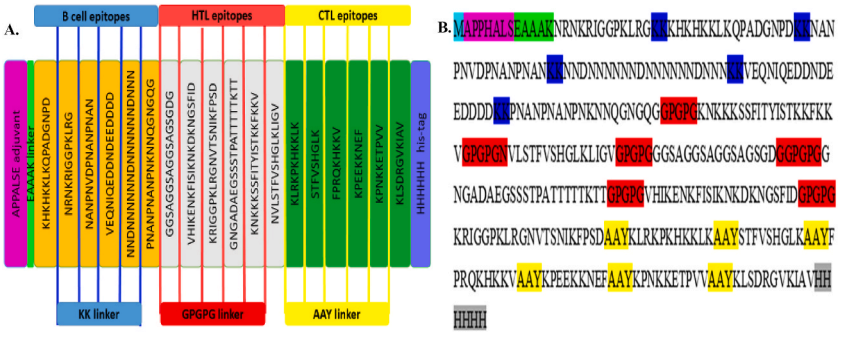

Fig. 1. Primary structure of PfCTMAG (A) Schematic view (B) Linear sequence.

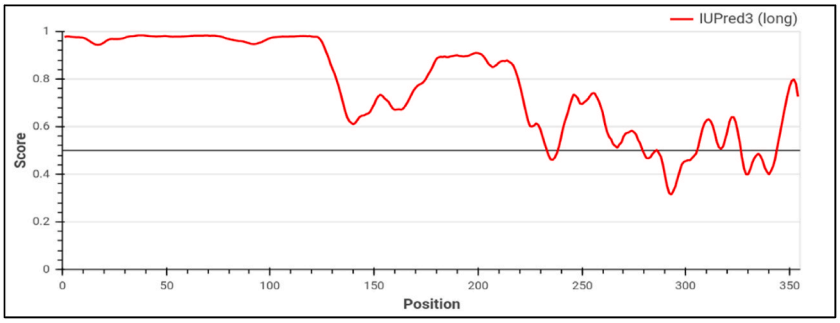

Fig. 2. Disordered regions predicted by IUpred3 showing a majority of residues located above the threshold score.

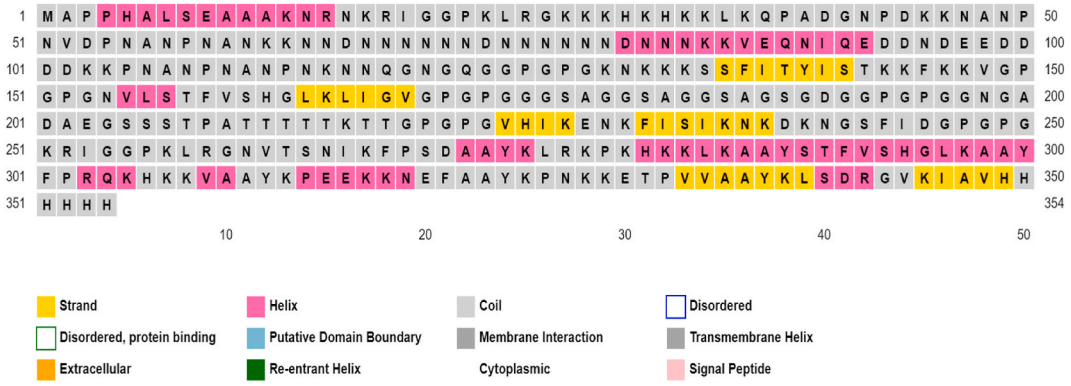

Fig. 3. Secondary structure predicted by PSIPRED mostly composed of grey residues which indicate coils.

3.1.11. Discontinuous B cell epitopes

PfCTMAG was predicted to contain nine conformational B-cell epitopes with scores ranging from 0.525 to 0.798 and sizes from 3 to 95 residues further validating its potential to trigger B cell immune responses.

3.1.12. Molecular docking

Docking of the PfCTMAG refined 3D structure with TLR4, MHCI, and MHCII generated 20 top solutions each with PatchDock. FireDock refined, rescored, and ranked the top 10 solutions in order of decreasing global energy. Solution 5 (TLR4), 2 (MHCI), and 9 (MHCII) were selected since they had the lowest energies. The interactions in the docked complex were visualized using PDBsum which showed the formation of 8 hydrogen bonds with TLR4, 16 with MHCI, and 14 with MHCII, as well as 5, 4, and 7 salt bridges respectively indicating a strong interaction. A high amount of non-bonded contacts was also observed in each docked complex (Supplementary materials Fig. S2).

3.1.13. Molecular dynamics simulation

This was done to confirm the flexibility of the docked complexes and the simulation results (Supplementary materials Fig. S3), the docked complexes were flexible on the basis of favourable B factor values, Eigenvalues, co-variances, and elastic models. PfCTMAG-

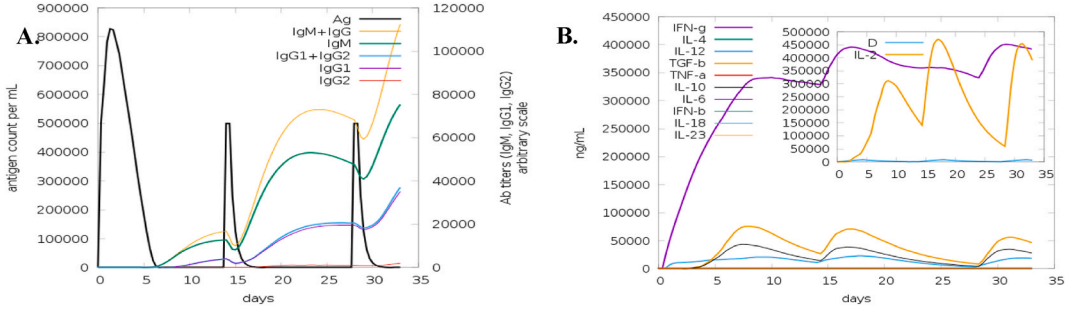

Fig. 4. Immune profile of PfCTMAG (A)Antigens and antibodies (B) Cytokines and Interleukins.

TLR4, PfCTMAG-MHCI and PfCTMAG-MHCII complexes had low eigenvalues of 1.3 x 10^{-5}, 1.6x 10^{-4} and 1.5 x 10^{-4} respectively.

3.1.14. Immune simulation

Following the primary injection, the antigen count per mL of PfCTMAG increased from day 0 with a peak count observed on day 2 and gradually decreased until day 6 (Fig. 4A). Subsequently, a strong antibody response, involving increased levels of both IgM and IgG was observed (Fig. 4B). Subsequent immune responses were found to be more robust than the primary response, resulting in significant antibody production and antigen clearance. This pattern aligns with a typical immune response, where repeated exposure to the antigen enhances immunity. The vaccination not only enhanced humoral immunity but also boosted cell-mediated immunity with increased B-cells (memory and plasma B-cells) and T-cells (cytotoxic and helper T-cells). PfCTMAG demonstrated the ability to effectively process and present antigens, as indicated by the heightened concentration of APCs, such as dendritic cells and macrophages following injection. Moreover, the levels of interferon-gamma and interleukin-2 rose significantly, with frequent exposure to the antigen, sustaining their peak levels. Consequently, this led to an elevated number of TH cells and production of immunoglobulins, which play a central role in triggering the humoral immune response (Supplementary materials Fig. S4).

3.1.15. Codon optimization and in silico cloning

This was performed using *E. coli* strain-K12 as the expression system, which gave a resulting improved sequence with a favourable GC content of 47.87 % and Codon Adaptation Index of 1 reflecting a high probability of effective expression in the selected host. A plasmid map of the final clone was generated consisting of 6318 bp of DNA including the PfCTMAG sequence (1080 bp).

3.1.16. Expression and purification

PfCTMAG was purified from inclusion bodies with a purity >70 % by SDS-PAGE (Fig. 5A) and a final protein concentration of 0.48 mg/mL. The quality check performed after receiving the candidate from GenScript validated its presence and integrity (Fig. 5B).

3.2. Assessment of seroreactivity in cases and controls

3.2.1. Demographic data of sampled population

A total of 350 participants (175 cases and 175 controls) were enrolled and their data recorded (Supplementary materials Table S4).

3.2.2. Determination of antigen and plasma dilutions for IgG and IgM

Plots of OD values against plasma dilutions for plates coated with different antigen concentrations indicated that an antigen concentration of 2.5 μg/mL and a plasma dilution of 1:250 are optimal for the measurement of IgG and IgM(Supplementary materials Figure S5).

3.2.3. Anti-PfCTMAG-IgM and -IgG levels and seropositivity in cases and controls

The [mean ± SD] IgG (0.149 ± 0.161) and IgM (0.412 ± 0.359) were higher ($p <$ **0.001** each) in cases than for controls (0.071 ± 0.082 vs 0.131 ± 0.122) (Fig. 6A). The overall seropositivity for IgG and IgM was 61.4 % and 89.7 % respectively (Fig. 6B). Cases were more seropositive for both IgG ($p =$ **0.024**) and IgM ($p <$ **0.001**) compared to controls. The seropositivity of IgG and IgM was further compared between cases and controls based on their demographic characteristics. There was an association between IgG and IgM seropositivity and clinical groups as shown in Supplementary materials Table S5 and Supplementary materials Table S6 respectively.

3.3. Safety and immunogenicity in animal model

3.3.1. Safety: animal weight gain toxicity test

During the 7-day post-immunization observation period, none of the mice died or displayed any signs of abnormality or ill health. Animal weight change test demonstrated that the mice immunized with PfCTMAG experienced a significant increase in weight, exceeding 60 % when compared to the control group (Supplementary materials Table S7). On day 3, there was no difference in mean

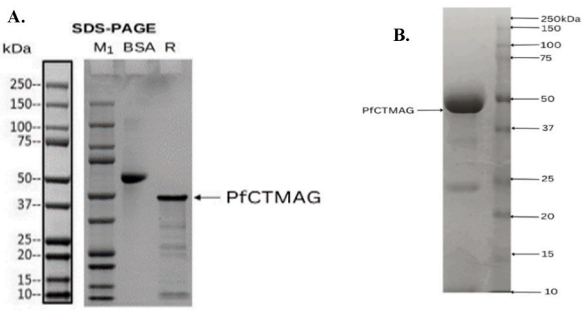

Fig. 5. SDS-PAGE Gels: Gel obtained by GenScript after expression and purification (A). Gel obtained from quality check after receiving the candidate from GenScript (B). The full non-adjusted gel images are available as supplementary material 'Gel Fig. 5A' and 'Gel Fig. 5B' respectively.

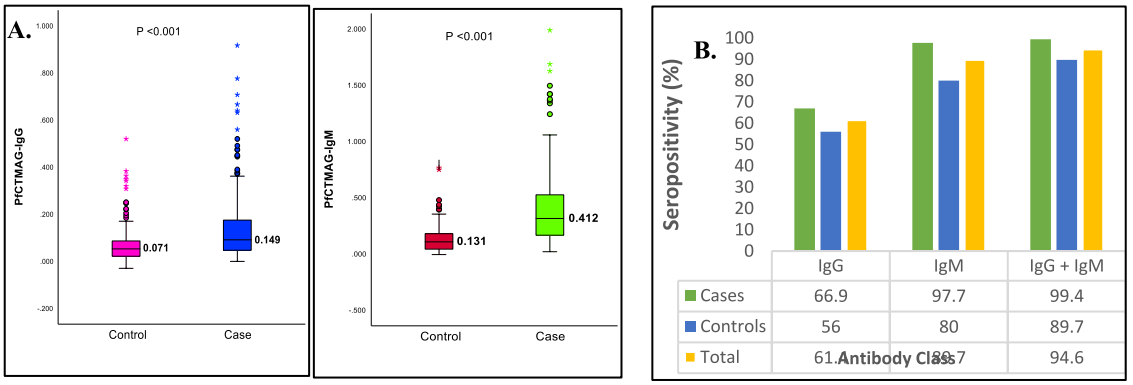

Fig. 6. Mean Anti-PfCTMAG IgG and IgM (A) Anti-PfCTMAG IgG and IgM seropositivity of cases and controls (B).

weight gain between the prime and control group but the control had a higher ($p = \mathbf{0.018}$) mean weight gain than the booster group. On day 7, no significant difference was observed in the weight gain among the groups.

3.3.2. *Immunogenicity assessment*

On day 0, IgG and IgM levels were similar among the different groups. There was a significant difference in IgG levels between the three groups on day 14 ($p = \mathbf{0.005}$) and 28 ($p = \mathbf{0.002}$) with higher levels in the prime (Fig. 7A) and booster (Fig. 7B) compared to the control group. For IgM, there was an increase from day 0–14 followed by a decrease to day 28 in the prime group compared to the control group (Fig. 7C) while the booster had a constant increase from day 0–28 (Fig. 7D). However, the IgM difference was not statistically significant across groups on day 14 ($p = 0.370$) and 28 ($p = 0.082$).

None of the mice in the control group were seropositive on days 0, 14, and 28. On day 14, there was a significant difference in the proportion of IgG seropositivity among groups ($p = 0.021$) with the highest proportion in the Booster ($p = 0.008$) compared to the control and no significant difference between the prime and control. On day 28, there was equally a significant difference in the number of IgG seropositivity between groups ($p = 0.001$) with higher number in the Prime ($p = 0.015$) and Booster ($p = 0.001$) compared to the control. For IgM, there was no significant difference in the seropositivity between groups on day 14 but there was a significant difference observed between groups on day 28 ($p = 0.002$) with the booster group significantly higher than both the Control

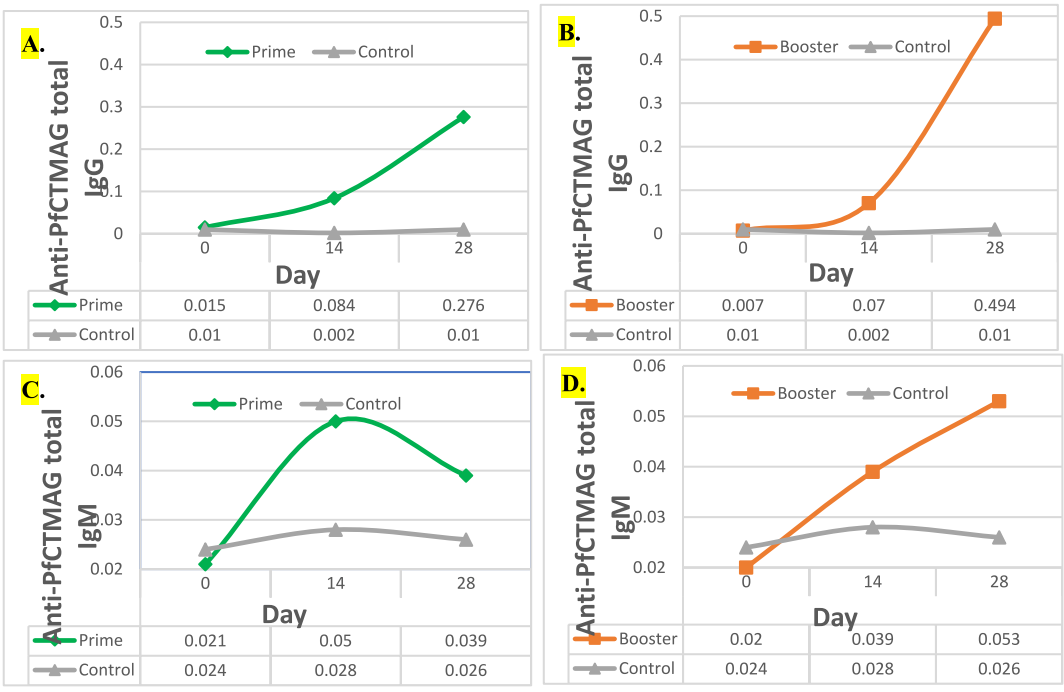

Fig. 7. Mean IgG levels of Prime vs Control (A), Booster vs Control (B), and Mean IgM of Prime vs Control (C), Booster vs Control (D) Groups Across Days.

($p = 0.002$) and Prime ($p = 0.030$) groups, while the Prime group did not significantly differ from the Control group (Fig. 8).

4. Discussion

With the advancement of multi-omics technology, the limitations associated with conventional vaccine development can be mitigated by coupling reverse vaccinology with immuno-informatics, in which web-based servers and specialized computer programs are employed to access, explore, and screen specific sequences of antigens (epitopes) that play a crucial role in triggering immune responses [68]. These predicted epitopes are then linked together to form multi-epitope vaccine (MEV) candidates. Few MEVs have been designed against *P. falciparum* [69–73]. However, these candidates have either focused on antigens present in a single stage of the life cycle or are based on antigens different from those identified in this study to have high antigenicity scores. Additionally, these candidates have not been evaluated *in vitro* and *in vivo*.

Given that signal peptides can impact protein folding and transport [74], they were cleaved from the selected antigens. Furthermore, transmembrane helices (TMHs) pose challenges in terms of cloning, expression, and purification as these TMHs are not exposed to the immune system [75] hence these helices were equally cleaved. Due to the significance of humoral immune responses mediated by B-cells and their antibody products, LBL epitopes were predicted in all antigens and assessed in terms of antigenicity, allergenicity, and toxicity. Cytotoxic T Lymphocyte epitopes recognize foreign antigens on MHC-I molecules subsequently destroying target cells, while HTL (MHC II binding) epitopes are important for both humoral and cell-mediated immune responses [76]. Therefore, CTL epitopes of all chosen antigens were predicted for A2, A3, and B7 alleles, which collectively cover approximately 88 % of the world's population [77]. Binding affinity is indicated by IC50 scores with scores <50 nM denoting higher affinity [78]. As such, only strong binders were considered and epitopes with the same core merged. Conservation among pathogen species is a characteristic of good vaccine candidates to promote cross-protection [79]. A BLAST search and epitope conservancy analysis of selected proteins and epitopes demonstrated a good degree of conservation in *P. vivax, P. knowlesi, P. malariae,* and *P. ovale*. The KK linkers help to decrease junctional immunogenicity [80], and AAY and GPGPG linkers exhibit a superior ability to present epitopes and provide optimal sites for proteasomal system cleavage [81–83]. Multi-epitope vaccines tend to induce relatively weak immune responses when used alone hence, adjuvants are added to improve their immunogenicity [84]. The PfCTMAG was augmented with the RS09 adjuvant at the N-terminal. The EAAAK linker enhances the interaction between the adjuvant and its receptor, ultimately increasing the bioactivity of the protein [85]. A high number of IFN-γ, IL-10-, and IL-4-inducing epitopes were predicted in PfCTMAG. IFN-γ and IL-4 are two important cytokines involved in immune response [86]. Initially, many candidates were designed with different built-in adjuvants but the one with RS09 had the greatest antigenicity score indicating its ability to trigger a strong immune response. The PfCTMAG was thus more antigenic than previously designed malaria MEVs with antigenicities of 1.181 [72], 0.5247 [70], and 0.5600 [71], 1.01 [73]. PfCTMAG was shown to be safe, non-allergenic, and non-toxigenic. The physicochemical features foreseen for PfCTMAG strongly support the feasibility of heterologous expression and antigen purification. The higher the aliphatic index the greater the thermostability [87], this implies PfCTMAG with an aliphatic index of 45.28 is only thermostable over a short range of temperatures. Stability was further evaluated through the instability index, with proteins considered stable if their index is below 40 [88]. Positive and negative GRAVY (Grand Average of Hydropathy) values represent the hydrophobic and hydrophilic qualities of a substance respectively [89]. Short half-lives often indicate instability [90] and better solubility of the recombinant protein within the *E. coli* host leads to more effective separation and purification upon expression [91] indicating that PfCTMAG was stable and expressible as denoted by the long half-life and high solubility score. The secondary structure analysis revealed that random coils were the most frequent secondary structure followed by extended strands, alpha helices and beta turns. These random coils are predominantly found on the protein's surface, protruding as flexible structures that may serve as potential epitopes for identification [92]. Validation is a crucial step in evaluating stability and identifying any inherent errors in the predicted 3D protein models [93]. An ERRAT score >50, indicates a good quality protein structure [94]. In order to effectively trigger an immune response, MEVs must possess a strong binding affinity with TLRs and docking predicts interactions amongst biological molecules such as a ligand with its receptor [95]. Numerous docked complexes were generated, and the complex with the lowest binding energy was selected for further analysis, as lower binding energies indicate stronger binding affinities [96]. The MD simulation graph demonstrated that the protein-protein combination remains highly stable, with minimal deformation observed in each residue. The eigenvalue serves as a crucial indicator of motion rigidity, a low eigenvalue signifies structures that possess a remarkable susceptibility to deformation [59,97]. Immune profiling is important in

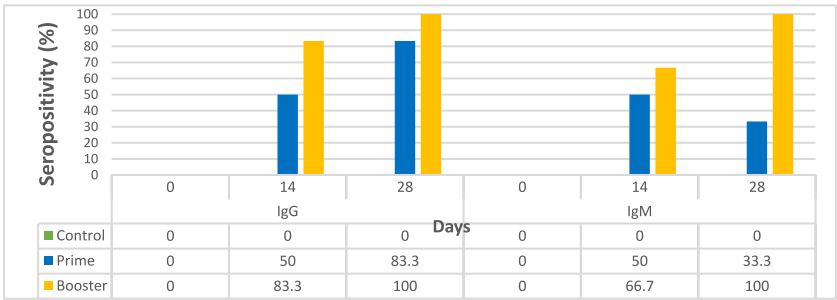

Fig. 8. Seropositivity of PfCTMAG IgG and IgM across mice treatment groups on days 0, 14, and 28.

determining a vaccine candidate's ability to trigger an immune response [98] and PfCTMAG induced a very high immune response *in silico*. Finally, to successfully produce a recombinant vaccine construct, it is crucial to select an appropriate heterologous system for expression.

The mean anti-PfCTMAG IgG and IgM levels were significantly higher in cases compared to controls which is an indication that a more robust immune response was present in individuals with current *P. falciparum* infection. Additionally, both cases and controls exhibited high seropositivity for IgG and IgM antibodies against PfCTMAG, with a slightly higher percentage observed in cases. This suggests that a larger proportion of individuals with malaria had greater exposure to the different components of the PfCTMAG antigen and developed detectable antibodies. The presence of anti-PfCTMAG antibodies in uninfected individuals can be attributed to various factors such as clearance of asymptomatic infection by the immune system [99], low levels of malaria parasites not detectable by microscopy or mRDT [100] and cross-reaction with antigens from other related parasites [101].

Ensuring vaccine safety is of utmost importance. However, it is crucial to recognize that no biological or pharmaceutical product, regardless of its development and production, can ever be considered completely safe [102]. It is recommended that the evaluation of safety should rely on clinical reactions and the weight gain of vaccinated animals compared to unvaccinated controls [103]. To investigate the safety of a vaccine by the animal weight change test, firstly, it should not cause a decline in mice weights three days after vaccination. Secondly, it should result in a weight gain of at least 60 % compared to the control group 7days post-vaccination. Lastly, the vaccine should not lead to more than 5 % mortality during the seven-day observation period, nor should it exhibit any signs of illness in the animals [104,105] and PFCTMAG fulfilled all the above criteria. The differences in weight gain among the groups observed on day 3 with the control group exhibiting the highest weight gain compared to all other groups, indicates that PfCTMAG did indeed simulate an actual infection, triggering an immune response that slowed metabolism in the mice [106] but this decrease was not significant enough to be considered toxic. On day 7, no significant differences in weight gain were observed among the groups. This could indicate a potential plateau effect or a convergence in weight gain between the different groups over time. The interpretation of these results is in line with previous studies assessing the safety of childhood vaccines in mice [107,108]. For immunogenicity assessment, the absence of statistically significant differences in IgG and IgM levels between the groups at the beginning of the experiment (day 0) suggests that any subsequent disparities in antibody levels observed at a later time are likely a result of the immunization rather than inherent distinctions between the groups. On day 14, both the prime and booster groups exhibited significantly higher IgG levels compared to the control implying that the immune system was successfully triggered by PfCTMAG, consistent with previous studies in which mice IgG levels rose after immunization with AARP [109], MSP2 [110] and CSP [111]. The lack of difference in IgG levels between the prime and booster groups is expected since they received the same dose on day 0. Conversely, IgM levels in the prime and booster groups were similar to controls. This deviates from previous studies that have demonstrated high levels of IgM upon immunization with malaria antigens [112]. This could be due to the fact that either the induced IgM response had subsided over 14 days or may not have been significantly influenced by the immunization. On day 28, the significant difference in IgG levels among all groups indicates a sustained effect on the immune response, suggesting that the vaccination was successful in inducing a lasting antibody response. Similar to day 14, there was no significant difference in IgM levels of all three groups. The lack of a significant difference between the prime and booster groups indicates that the booster dose administered on day 14 did not significantly enhance the immune response induced by the prime dose. This suggests that the prime immunization alone was effective in eliciting a strong immune response. It is also important to note that induction of IgG and IgM immune response in some cases might result from an actual infection rather than from the vaccine candidate and vaccine-induced immune response can often be differentiated from an immune response induced by natural infection [113].

5. Conclusion

The integration of reverse vaccinology with immunoinformatics led to the design of a promising multi-epitope vaccine candidate, PfCTMAG, against *P. falciparum*. This candidate demonstrates strong antigenicity, safety, and the potential for a robust immune response, as indicated by significant IgG and IgM levels in infected mice. While PfCTMAG shows encouraging results, further *in vitro* and *in vivo* evaluations are essential to confirm its efficacy and optimize its application in malaria prevention. Therefore, in future studies, we plan to compare the immune response of PfCTMAG against other approved malaria vaccines, investigate the optimal dose regimen, evaluate the immune response when combined with different external adjuvants, and also test the DNA construct of PfCTMAG.

CRediT authorship contribution statement

Joan A. Chick: Writing – original draft, Resources, Project administration, Methodology, Investigation, Data curation, Conceptualization. **Nadege N. Abongdia:** Writing – review & editing, Resources, Methodology, Investigation, Data curation. **Robert A. Shey:** Writing – review & editing, Validation, Supervision, Resources, Methodology. **Tobias O. Apinjoh:** Writing – review & editing, Validation, Supervision, Resources, Formal analysis, Conceptualization.

Informed consent statement

All participants provided written informed consent to participate in the study and for their data to be published.

Ethical statement

This study was approved by the Institutional Review Board of the Faculty of Health Science, The University of Bamenda (2023/0869H/UBa/IRB). The clearance for animal studies was obtained from the University of Buea Institutional Animal Care and Use Committee, (UB-IACUC No 20/2023).

Data availability statement

The original contributions presented in the study are included in the article/supplementary material, further inquiries can be directed to the corresponding author.

Funding

This research received no external funding.

Declaration of competing interest

The authors declare that they have no known competing financial interests or personal relationships that could have appeared to influence the work reported in this paper.

Acknowledgments

Professor Fidelis Cho-Ngwa, head of the Laboratory for Drugs and Molecular Diagnostics, and Professor Stephen M. Ghogomu, head of the Molecular and Cell Biology Laboratory at the University of Buea, for laboratory space and materials used for experiments.

Appendix A. Supplementary data

Supplementary data to this article can be found online at https://doi.org/10.1016/j.heliyon.2025.e42014.

References

[1] World Health Organization, World Malaria Report 2022, License: CC BY-NC-SA 3.0 IGO, Geneva, 2022.
[2] R.M. Fairhurst, G.M.L. Nayyar, J.G. Breman, R. Hallett, J.L. Vennerstrom, S. Duong, P. Ringwald, T.E. Wellems, C.V. Plowe, A.M. Dondorp, Artemisinin-resistant malaria: research challenges, opportunities, and public health implications, Am. J. Trop. Med. Hyg. 87 (2) (2012) 231–241, https://doi.org/10.4269/ajtmh.2012.12-0025.
[3] W.L. Mandala, V. Harawa, F. Dzinjalamala, D. Tembo, The role of different components of the immune system against *Plasmodium* falciparum malaria: possible contribution towards malaria vaccine development, Mol. Biochem. Parasitol. 246 (2021) 111425, https://doi.org/10.1016/j.molbiopara.2021.111425.
[4] C. Aguttu, B.A. Okech, A. Mukisa, G.W. Lubega, Screening and characterization of hypothetical proteins of *Plasmodium* falciparum as novel vaccine candidates in the fight against malaria using reverse vaccinology, J. Genet. Eng. Biotechnol. 19 (1) (2021) 103, https://doi.org/10.1186/s43141-021-00199-y.
[5] P.E. Duffy, J. Patrick Gorres, Malaria vaccines since 2000: progress, priorities, products, NPJ vaccines 5 (1) (2020) 48, https://doi.org/10.1038/s41541-020-0196-3.
[6] WHO. World malaria report, 20 Years of Global Progress and Challenges, World Health Organiation, Geneva, Switzerland, 2020, 2020.
[7] M.T. White, R. Verity, J.T. Griffin, K.P. Asante, S. Owusu-Agyei, B. Greenwood, C. Drakeley, S. Gesase, J. Lusingu, D. Ansong, S. Adjei, T. Agbenyega, B. Ogutu, L. Otieno, W. Otieno, S.T. Agnandji, B. Lell, P. Kremsner, I. Hoffman, F. Martinson, A.C. Ghani, Immunogenicity of the RTS,S/AS01 malaria vaccine and implications for duration of vaccine efficacy: secondary analysis of data from a phase 3 randomised controlled trial, Lancet Infect. Dis. 15 (12) (2015) 1450–1458, https://doi.org/10.1016/S1473-3099(15)00239-X.
[8] WHO recommends R21/Matrix-M vaccine for malaria prevention in updated advice on immunization, Available at, https://www.who.int/news/item/02-10-2023-who-recommends-r21-matrix-m-vaccine-for-malaria-prevention-in-updated-advice-on-immunization. (Accessed 5 October 2023).
[9] P. Zimmermann, N. Curtis, Factors that influence the immune response to vaccination, Clin. Microbiol. Rev. 32 (2) (2019) e00084, https://doi.org/10.1128/CMR.00084-18.
[10] R. Rappuoli, Reverse vaccinology, Curr. Opin. Microbiol. 3 (5) (2000) 445–450, https://doi.org/10.1016/s1369-5274(00)00119-3.
[11] S.S. Usmani, R. Kumar, S. Bhalla, V. Kumar, G.P.S. Raghava, *In silico* tools and databases for designing peptide-based vaccine and drugs, Advances in protein chemistry and structural biology 112 (2018) 221–263, https://doi.org/10.1016/bs.apcsb.2018.01.006.
[12] B.E. Correia, J.T. Bates, R.J. Loomis, G. Baneyx, C. Carrico, J.G. Jardine, P. Rupert, C. Correnti, O. Kalyuzhniy, V. Vittal, M.J. Connell, E. Stevens, A. Schroeter, M. Chen, S. Macpherson, A.M. Serra, Y. Adachi, M.A. Holmes, Y. Li, R.E. Klevit, W.R. Schief, Proof of principle for epitope-focused vaccine design, Nature 507 (7491) (2014) 201–206, https://doi.org/10.1038/nature12966.
[13] Y. Feng, H. Jiang, M. Qiu, L. Liu, S. Zou, Y. Li, Q. Guo, N. Han, Y. Sun, K. Wang, L. Lu, X. Zhuang, S. Zhang, S. Chen, F. Mo, Multi-epitope vaccine design using an immunoinformatic approach for SARS-CoV-2, Pathogens 10 (6) (2021) 737, https://doi.org/10.3390/pathogens10060737.
[14] M.M. Shehata, S.H. Mahmoud, M. Tarek, A.A. Al-Karmalawy, A. Mahmoud, A. Mostafa, M. M Elhefnawi, M.A. Ali, *In silico* and in vivo evaluation of SARS-CoV-2 predicted epitopes-based candidate vaccine, Molecules 26 (20) (2021) 6182, https://doi.org/10.3390/molecules26206182.
[15] A. Atapour, P. Vosough, S. Jafari, G.A. Sarab, A multi-epitope vaccine designed against blood-stage of malaria: an immunoinformatic and structural approach, Sci. Rep. 12 (1) (2022) 11683, https://doi.org/10.1038/s41598-022-15956-3.
[16] P.C. Callaway, L.A. Farrington, M.E. Feeney, Malaria and early life immunity: competence in context, Front. Immunol. 12 (2021) 634749, https://doi.org/10.3389/fimmu.2021.634749.
[17] Britanica, Climate of Cameroon. https://www.britannica.com/place/Cameroon/Climate, 2023. (Accessed 12 February 2023).

[18] P.N. Kwi, E.E. Ewane, M.N. Moyeh, L.N. Tangi, V.N. Ntui, F. Zeukeng, D.D. Sofeu-Feugaing, E.A. Achidi, F. Cho-Ngwa, A. Amambua-Ngwa, J.D. Bigoga, T. O. Apinjoh, Diversity and behavioral activity of Anopheles mosquitoes on the slopes of Mount Cameroon, Parasites Vectors 15 (1) (2022) 344, https://doi.org/10.1186/s13071-022-05472-8.

[19] I. Nebie, A. Diarra, A. Ouedraogo, I. Soulama, E.C. Bougouma, A.B. Tiono, A.T. Konate, R. Chilengi, M. Theisen, D. Dodoo, E. Remarque, S. Bosomprah, P. Milligan, S.B. Sirima, Humoral responses to *Plasmodium* falciparum blood-stage antigens and association with incidence of clinical malaria in children living in an area of seasonal malaria transmission in Burkina Faso, West Africa, Infect. Immun. 76 (2) (2008) 759–766, https://doi.org/10.1128/IAI.01147-07.

[20] W.N. Arifin, W.M. Zahiruddin, Sample size calculation in animal studies using resource equation approach, Malays. J. Med. Sci. : MJMS 24 (5) (2017) 101–105, https://doi.org/10.21315/mjms2017.24.5.11.

[21] V. Thumuluri, J.J. Almagro Armenteros, A.R. Johansen, H. Nielsen, O. Winther, DeepLoc 2.0: multi-label subcellular localization prediction using protein language models, Nucleic Acids Res. 50 (W1) (2022) W228–W234, https://doi.org/10.1093/nar/gkac278.

[22] P. Horton, K.J. Park, T. Obayashi, N. Fujita, H. Harada, C.J. Adams-Collier, K. Nakai, WoLF PSORT: protein localization predictor, Nucleic Acids Res. 35 (Web Server issue) (2007) W585–W587, https://doi.org/10.1093/nar/gkm259.

[23] F. Teufel, J.J. Almagro Armenteros, A.R. Johansen, M.H. Gíslason, S.I. Pihl, K.D. Tsirigos, O. Winther, S. Brunak, G. von Heijne, H. Nielsen, SignalP 6.0 predicts all five types of signal peptides using protein language models, Nat. Biotechnol. 40 (7) (2022) 1023–1025, https://doi.org/10.1038/s41587-021-01156-3.

[24] K. Hiller, A. Grote, M. Scheer, R. Münch, D. Jahn, PrediSi: prediction of signal peptides and their cleavage positions, Nucleic Acids Res. 32 (Web Server issue) (2004) W375–W379, https://doi.org/10.1093/nar/gkh378.

[25] A. Krogh, B. Larsson, G. von Heijne, E.L. Sonnhammer, Predicting transmembrane protein topology with a hidden Markov model: application to complete genomes, J. Mol. Biol. 305 (3) (2001) 567–580, https://doi.org/10.1006/jmbi.2000.4315.

[26] K.D. Tsirigos, C. Peters, N. Shu, L. Käll, A. Elofsson, The TOPCONS web server for consensus prediction of membrane protein topology and signal peptides, Nucleic Acids Res. 43 (W1) (2015) W401–W407, https://doi.org/10.1093/nar/gkv485.

[27] M.C. Jespersen, B. Peters, M. Nielsen, P. Marcatili, BepiPred-2.0: improving sequence-based B-cell epitope prediction using conformational epitopes, Nucleic Acids Res. 45 (W1) (2017) W24–W29, https://doi.org/10.1093/nar/gkx346.

[28] B. Yao, L. Zhang, S. Liang, C. Zhang, SVMTriP: a method to predict antigenic epitopes using support vector machine to integrate tri-peptide similarity and propensity, PLoS One 7 (9) (2012) e45152, https://doi.org/10.1371/journal.pone.0045152.

[29] K. Rawal, R. Sinha, B.A. Abbasi, A. Chaudhary, S.K. Nath, P. Kumari, P. Preeti, D. Saraf, S. Singh, K. Mishra, P. Gupta, A. Mishra, T. Sharma, S. Gupta, P. Singh, S. Sood, P. Subramani, A.K. Dubey, U. Strych, P.J. Hotez, M.E. Bottazzi, Identification of vaccine targets in pathogens and design of a vaccine using computational approaches, Sci. Rep. 11 (1) (2021) 17626, https://doi.org/10.1038/s41598-021-96863-x.

[30] A. Sette, J. Sidney, Nine major HLA class I supertypes account for the vast preponderance of HLA-A and -B polymorphism, Immunogenetics 50 (3–4) (1999) 201–212, https://doi.org/10.1007/s002510050594.

[31] S. Lata, M. Bhasin, G.P. Raghava, Application of machine learning techniques in predicting MHC binders, Methods Mol. Biol. 409 (2007) 201–215, https://doi.org/10.1007/978-1-60327-118-9_14.

[32] I.A. Doytchinova, D.R. Flower, VaxiJen: a server for prediction of protective antigens, tumour antigens and subunit vaccines, BMC Bioinf. 8 (2007) 4, https://doi.org/10.1186/1471-2105-8-4.

[33] M.A. Rasheed, S. Raza, A. Zohaib, M.I. Riaz, A. Amin, M. Awais, S.U. Khan, M. Ijaz Khan, Y.M. Chu, Immunoinformatics based prediction of recombinant multi-epitope vaccine for the control and prevention of SARS-CoV-2, Alex. Eng. J. 60 (3) (2021) 3087–3097.

[34] I. Dimitrov, I. Bangov, D.R. Flower, I. Doytchinova, AllerTOP v.2–a server for *in silico* prediction of allergens, J. Mol. Model. 20 (6) (2014) 2278, https://doi.org/10.1007/s00894-014-2278-5.

[35] I. Dimitrov, L. Naneva, I. Doytchinova, I. Bangov, AllergenFP: allergenicity prediction by descriptor fingerprints, Bioinformatics 30 (6) (2014) 846–851, https://doi.org/10.1093/bioinformatics/btt619.

[36] S. Gupta, P. Kapoor, K. Chaudhary, A. Gautam, R. Kumar, Open Source Drug Discovery Consortium, & Raghava, G. P., *In silico* approach for predicting toxicity of peptides and proteins, PLoS One 8 (9) (2013) e73957, https://doi.org/10.1371/journal.pone.0073957.

[37] S.F. Altschul, W. Gish, W. Miller, E.W. Myers, D.J. Lipman, Basic local alignment search tool, J. Mol. Biol. 215 (3) (1990) 403–410, https://doi.org/10.1016/S0022-2836(05)80360-2.

[38] H.H. Bui, J. Sidney, W. Li, N. Fusseder, A. Sette, Development of an epitope conservancy analysis tool to facilitate the design of epitope-based diagnostics and vaccines, BMC Bioinf. 8 (2007) 361, https://doi.org/10.1186/1471-2105-8-361.

[39] A. Shanmugam, S. Rajoria, A.L. George, A. Mittelman, R. Suriano, R.K. Tiwari, Synthetic Toll like receptor-4 (TLR-4) agonist peptides as a novel class of adjuvants, PLoS One 7 (2) (2012) e30839, https://doi.org/10.1371/journal.pone.0030839.

[40] E. Gasteiger, C. Hoogland, A. Gattiker, S. Duvaud, M.R. Wilkins, R.D. Appel, A. Bairoch, Protein identification and analysis tools on the ExPASy server, in: J. M. Walker (Ed.), The Proteomics Protocols Handbook, Humana Press, New York, 2005, pp. 571–607.

[41] C.N. Magnan, A. Randall, P. Baldi, SOLpro: accurate sequence-based prediction of protein solubility, Bioinformatics 25 (17) (2009) 2200–2207, https://doi.org/10.1093/bioinformatics/btp386.

[42] S.K. Dhanda, P. Vir, G.P. Raghava, Designing of interferon-gamma inducing MHC class-II binders, Biol. Direct 8 (2013) 30, https://doi.org/10.1186/1745-6150-8-30.

[43] S.K. Dhanda, S. Gupta, P. Vir, G.P. Raghava, Prediction of IL4 inducing peptides, Clin. Dev. Immunol. 2013 (2013) 263952, https://doi.org/10.1155/2013/263952.

[44] G. Nagpal, S.S. Usmani, S.K. Dhanda, H. Kaur, S. Singh, M. Sharma, G.P. Raghava, Computer-aided designing of immunosuppressive peptides based on IL-10 inducing potential, Sci. Rep. 7 (2017) 42851, https://doi.org/10.1038/srep42851.

[45] D.W.A. Buchan, D.T. Jones, The PSIPRED protein analysis workbench: 20 years on, Nucleic Acids Res. 47 (W1) (2019) W402–W407, https://doi.org/10.1093/nar/gkz297.

[46] C. Geourjon, G. Deléage, SOPMA: significant improvements in protein secondary structure prediction by consensus prediction from multiple alignments, Comput. Appl. Biosci. : CABIOS 11 (6) (1995) 681–684, https://doi.org/10.1093/bioinformatics/11.6.681.

[47] G. Corradin, V. Villard, A.V. Kajava, Protein structure based strategies for antigen discovery and vaccine development against malaria and other pathogens, Endocr. Metab. Immune Disord. - Drug Targets 7 (4) (2007) 259–265, https://doi.org/10.2174/187153007782794371.

[48] A.J. Guy, V. Irani, C.A. MacRaild, R.F. Anders, R.S. Norton, J.G. Beeson, J.S. Richards, P.A. Ramsland, Insights into the immunological properties of intrinsically disordered malaria proteins using proteome scale predictions, PLoS One 10 (10) (2015) e0141729, https://doi.org/10.1371/journal.pone.0141729.

[49] G. Erdős, M. Pajkos, Z. Dosztányi, IUPred3: prediction of protein disorder enhanced with unambiguous experimental annotation and visualization of evolutionary conservation, Nucleic Acids Res. 49 (W1) (2021) W297–W303, https://doi.org/10.1093/nar/gkab408.

[50] J. Yang, Y. Zhang, I-TASSER server: new development for protein structure and function predictions, Nucleic Acids Res. 43 (W1) (2015) W174–W181, https://doi.org/10.1093/nar/gkv342.

[51] D. Xu, Y. Zhang, Improving the physical realism and structural accuracy of protein models by a two-step atomic-level energy minimization, Biophys. J. 101 (10) (2011) 2525–2534, https://doi.org/10.1016/j.bpj.2011.10.024.

[52] J. Ko, H. Park, L. Heo, C. Seok, GalaxyWEB server for protein structure prediction and refinement, Nucleic Acids Res. 40 (Web Server issue) (2012) W294–W297, https://doi.org/10.1093/nar/gks493.

[53] M. Wiederstein, M.J. Sippl, ProSA-web: interactive web service for the recognition of errors in three-dimensional structures of proteins, Nucleic Acids Res. 35 (Web Server issue) (2007) W407–W410, https://doi.org/10.1093/nar/gkm290.

[54] C. Colovos, T.O. Yeates, Verification of protein structures: patterns of nonbonded atomic interactions, Protein Sci. : a publication of the Protein Society 2 (9) (1993) 1511–1519, https://doi.org/10.1002/pro.5560020916.

[55] Roman Laskowski, M.W. Macarthur, D.S. Moss, Janet Thornton, PROCHECK: a program to check the stereochemical quality of protein structures, J. Appl. Crystallogr. 26 (1993) 283–291, https://doi.org/10.1107/S0021889892009944.

[56] J. Ponomarenko, H.H. Bui, W. Li, N. Fusseder, P.E. Bourne, A. Sette, B. Peters, ElliPro: a new structure-based tool for the prediction of antibody epitopes, BMC Bioinf. 9 (2008) 514, https://doi.org/10.1186/1471-2105-9-514.

[57] D. Schneidman-Duhovny, Y. Inbar, R. Nussinov, H.J. Wolfson, PatchDock and SymmDock: servers for rigid and symmetric docking, Nucleic Acids Res. 33 (Web Server issue) (2005) W363–W367, https://doi.org/10.1093/nar/gki481.

[58] N. Andrusier, R. Nussinov, H.J. Wolfson, FireDock: fast interaction refinement in molecular docking, Proteins 69 (1) (2007) 139–159, https://doi.org/10.1002/prot.21495.

[59] J.R. López-Blanco, J.I. Aliaga, E.S. Quintana-Ortí, P. Chacón, iMODS: internal coordinates normal mode analysis server, Nucleic Acids Res. 42 (Web Server issue) (2014) W271–W276, https://doi.org/10.1093/nar/gku339.

[60] N. Rapin, O. Lund, M. Bernaschi, F. Castiglione, Computational immunology meets bioinformatics: the use of prediction tools for molecular binding in the simulation of the immune system, PLoS One 5 (4) (2010) e9862.

[61] A. Grote, K. Hiller, M. Scheer, R. Münch, B. Nörtemann, D.C. Hempel, D. Jahn, JCat: a novel tool to adapt codon usage of a target gene to its potential expression host, Nucleic Acids Res. 33 (Web Server issue) (2005) W526–W531, https://doi.org/10.1093/nar/gki376.

[62] P.M. Sharp, W.H. Li, The codon Adaptation Index–a measure of directional synonymous codon usage bias, and its potential applications, Nucleic Acids Res. 15 (3) (1987) 1281–1295, https://doi.org/10.1093/nar/15.3.1281.

[63] E.A. Achidi, T.O. Apinjoh, E. Mbunwe, R. Besingi, C. Yafi, N. Wenjighe Awah, A. Ajua, J.K. Anchang, Febrile status, malarial parasitaemia and gastro-intestinal helminthiases in schoolchildren resident at different altitudes, in south-western Cameroon, Ann. Trop. Med. Parasitol. 102 (2) (2008) 103–118, https://doi.org/10.1179/136485908X252287.

[64] WHO, Giemsa staining of malaria blood films. Malaria Microscopy Standard Operating Procedure—MM-SOP-07a, World Health Organization, Geneva, Switzerland, 2016, pp. 1–6.

[65] WHO, Malaria Parasite Counting, vols. 1–5, World Health Organization, 2016.

[66] H. Guan, J. Peng, L. Jiang, G. Mo, X. Li, X. Peng, CD19+CD1dhiCD5hi B cells can downregulate malaria ITV protection by IL-10 secretion, Front. Public Health 8 (2020) 77, https://doi.org/10.3389/fpubh.2020.00077.

[67] S. Hauge, A. Madhun, R.J. Cox, L.R. Haaheim, Quality and kinetics of the antibody response in mice after three different low-dose influenza virus vaccination strategies, Clin. Vaccine Immunol. : CVI 14 (8) (2007) 978–983, https://doi.org/10.1128/CVI.00033-07.

[68] N.R. Hegde, S. Gauthami, H.M. Sampath Kumar, J. Bayry, The use of databases, data mining and immunoinformatics in vaccinology: where are we? Expet Opin. Drug Discov. 13 (2) (2018) 117–130, https://doi.org/10.1080/17460441.2018.1413088.

[69] Z. Zhou, C.W. Todd, R.M. Wohlhueter, A. Price, L. Xiao, P. Schnake, P.C. Bonner, A.M. Martin, I.F. Goldman, P. De La Vega, V. Udhayakumar, A.A. Lal, Development, characterization and immunogenicity of a multi-stage, multi-valent *Plasmodium* falciparum vaccine antigen (FALVAC-1A) expressed in Escherichia coli, Hum. Vaccine 2 (1) (2006) 14–23, https://doi.org/10.4161/hv.2.1.2437.

[70] R.K. Pandey, M. Ali, R. Ojha, T.K. Bhatt, V.K. Prajapati, Development of multi-epitope driven subunit vaccine in secretory and membrane protein of *Plasmodium* falciparum to convey protection against malaria infection, Vaccine 36 (30) (2018) 4555–4565, https://doi.org/10.1016/j.vaccine.2018.05.082.

[71] P. Bemani, Z. Amirghofran, M. Mohammadi, Designing a multi-epitope vaccine against blood-stage of *Plasmodium* falciparum by *in silico* approaches, J. Mol. Graph. Model. 99 (2020) 107645, https://doi.org/10.1016/j.jmgm.2020.107645.

[72] L. Maharaj, V.T. Adeleke, A.J. Fatoba, A.A. Adeniyi, S.I. Tshilwane, M.A. Adeleke, R. Maharaj, M. Okpeku, Immunoinformatics approach for multi-epitope vaccine design against *P. falciparum* malaria, Infection, genetics and evolution :journal of molecular epidemiology and evolutionary genetics in infectious diseases 92 (2021) 104875, https://doi.org/10.1016/j.meegid.2021.104875.

[73] M. Pritam, G. Singh, S. Swaroop, A.K. Singh, B. Pandey, S.P. Singh, A cutting-edge immunoinformatics approach for design of multi-epitope oral vaccine against dreadful human malaria, Int. J. Biol. Macromol. 158 (2020) 159–179, https://doi.org/10.1016/j.ijbiomac.2020.04.191.

[74] R. Lu, T. Zhang, S. Song, M. Zhou, L. Jiang, Z. He, Y. Yuan, T. Yuan, Y. Lu, K. Yan, Y. Cheng, Accurately cleavable goat β-lactoglobulin signal peptide efficiently guided translation of a recombinant human plasminogen activator in transgenic rabbit mammary gland, Biosci. Rep. 39 (6) (2019) BSR20190596, https://doi.org/10.1042/BSR20190596.

[75] G.P. Monterrubio-López, J.A. González-Y-Merchand, R.M. Ribas-Aparicio, Identification of novel potential vaccine candidates against tuberculosis based on reverse vaccinology, BioMed Res. Int. 2015 (2015) 483150, https://doi.org/10.1155/2015/483150.

[76] S.P. Kurup, N.S. Butler, J.T. Harty, T cell-mediated immunity to malaria, Nat. Rev. Immunol. 19 (7) (2019) 457–471, https://doi.org/10.1038/s41577-019-0158-z.

[77] V.S. Rajput, R. Sharma, A. Kumari, N. Vyas, V. Prajapati, A. Grover, Engineering a multi epitope vaccine against SARS-CoV-2 by exploiting its non structural and structural proteins, J. Biomol. Struct. Dynam. 40 (19) (2022) 9096–9113, https://doi.org/10.1080/07391102.2021.1924265.

[78] F.F. Albaqami, A. Altharawi, H.N. Althurwi, K.M. Alharthy, M. Qasim, Z.T. Muhseen, M. Tahir Ul Qamar, Computational modeling and evaluation of potential mRNA and peptide-based vaccine against marburg virus (MARV) to provide immune protection against hemorrhagic fever, BioMed Res. Int. 2023 (2023) 5560605, https://doi.org/10.1155/2023/5560605.

[79] M.M. Hester, L.V. Oliveira, R. Wang, Z. Mou, D. Lourenco, G.R. Ostroff, C.A. Specht, S.M. Levitz, Cross-reactivity between vaccine antigens from the chitin deacetylase protein family improves survival in a mouse model of cryptococcosis, Front. Immunol. 13 (2022) 1015586.

[80] A. Maleki, G. Russo, G.A. Parasiliti Palumbo, F. Pappalardo, *In silico* design of recombinant multi-epitope vaccine against influenza A virus, BMC Bioinf. 22 (Suppl 14) (2022) 617, https://doi.org/10.1186/s12859-022-04581-6.

[81] A. Rahmani, M. Baee, M. Rostamtabar, A. Karkhah, S. Alizadeh, M. Tourani, H.R. Nouri, Development of a conserved chimeric vaccine based on helper T-cell and CTL epitopes for induction of strong immune response against Schistosoma mansoni using immunoinformatics approaches, Int. J. Biol. Macromol. 141 (2019) 125–136, https://doi.org/10.1016/j.ijbiomac.2019.08.259.

[82] P.K. Yadalam, R.V. Anegundi, S. Munawar, R. Ramadoss, S. Rengaraj, S. Ramesh, M. Aljeldah, B.R.A. Shammari, A.A. Alshehri, A.S.S. Alwashmi, S. A. Turkistani, A. Alawfi, A. Alshengeti, M. Garout, A.A. Sabour, M.A. Alshiekheid, F.S. Aljebaly, A.A. Rabaan, Designing novel multi-epitope vaccine construct against *Prevotella intermedia*-interpain A: an immunoinformatics approach, Medicina (Kaunas, Lithuania) 59 (2) (2023) 302, https://doi.org/10.3390/medicina59020302.

[83] S. Sanami, S. Nazarian, S. Ahmad, E. Raeisi, M. Tahir Ul Qamar, S. Tahmasebian, H. Pazoki-Toroudi, M. Fazeli, M. Ghatreh Samani, *In silico* design and immunoinformatics analysis of a universal multi-epitope vaccine against monkeypox virus, PLoS One 18 (5) (2023) e0286224, https://doi.org/10.1371/journal.pone.0286224.

[84] M. Tahir Ul Qamar, S. Saleem, U.A. Ashfaq, A. Bari, F. Anwar, S. Alqahtani, Epitope-based peptide vaccine design and target site depiction against Middle East Respiratory Syndrome Coronavirus: an immune-informatics study, J. Transl. Med. 17 (1) (2019) 362, https://doi.org/10.1186/s12967-019-2116-8.

[85] R. Arai, H. Ueda, A. Kitayama, N. Kamiya, T. Nagamune, Design of the linkers which effectively separate domains of a bifunctional fusion protein, Protein Eng. 14 (8) (2001) 529–532, https://doi.org/10.1093/protein/14.8.529.

[86] F. Annunziato, L. Cosmi, F. Liotta, E. Maggi, S. Romagnani, Human Th1 dichotomy: origin, phenotype and biologic activities, Immunology 144 (3) (2014) 343–351, https://doi.org/10.1111/imm.12399. Advance online publication.

[87] A. Ikai, Thermostability and aliphatic index of globular proteins, J. Biochem. 88 (6) (1980) 1895–1898.

[88] D.G. Gamage, A. Gunaratne, G.R. Periyannan, T.G. Russell, Applicability of instability index for in vitro protein stability prediction, Protein Pept. Lett. 26 (5) (2019) 339–347, https://doi.org/10.2174/0929866526666190228144219.

[89] J. Kyte, R.F. Doolittle, A simple method for displaying the hydropathic character of a protein, J. Mol. Biol. 157 (1) (1982) 105–132.

[90] E.F. Fornasiero, J.N. Savas, Determining and interpreting protein lifetimes in mammalian tissues, Trends Biochem. Sci. 48 (2) (2023) 106–118, https://doi.org/10.1016/j.tibs.2022.08.011.

[91] H.P. Sørensen, K.K. Mortensen, Soluble expression of recombinant proteins in the cytoplasm of Escherichia coli, Microb. Cell Factories 4 (1) (2005) 1, https://doi.org/10.1186/1475-2859-4-1.
[92] Y. Wang, Bioinformatics analysis of NetF proteins for designing a multi-epitope vaccine against Clostridium perfringens infection, Infect. Genet. Evol. : journal of molecular epidemiology and evolutionary genetics in infectious diseases 85 (2020) 104461, https://doi.org/10.1016/j.meegid.2020.104461.
[93] N. Khatoon, R.K. Pandey, V.K. Prajapati, Exploring Leishmania secretory proteins to design B and T cell multi-epitope subunit vaccine using immunoinformatics approach, Sci. Rep. 7 (1) (2017) 8285.
[94] A. Messaoudi, H. Belguith, J. Ben Hamida, Homology modeling and virtual screening approaches to identify potent inhibitors of VEB-1 β-lactamase, Theor. Biol. Med. Model. 10 (2013) 22, https://doi.org/10.1186/1742-4682-10-22.
[95] T. Lengauer, M. Rarey, Computational methods for biomolecular docking, Curr. Opin. Struct. Biol. 6 (3) (1996) 402–406, https://doi.org/10.1016/s0959-440x(96)80061-3.
[96] X. Xu, C. Yan, X. Zou, Improving binding mode and binding affinity predictions of docking by ligand-based search of protein conformations: evaluation in D3R grand challenge 2015, J. Comput. Aided Mol. Des. 31 (8) (2017) 689–699, https://doi.org/10.1007/s10822-017-0038-1.
[97] S.B. Sayed, Z. Nain, M.S.A. Khan, F. Abdulla, R. Tasmin, U.K. Adhikari, Exploring lassa virus proteome to design a multi-epitope vaccine through immunoinformatics and immune simulation analyses, Int. J. Pept. Res. Therapeut. 26 (4) (2020) 2089–2107, https://doi.org/10.1007/s10989-019-10003-8.
[98] R.A. Shey, S.M. Ghogomu, C.M. Shintouo, F.N. Nkemngo, D.N. Nebangwa, K. Esoh, N.E. Yaah, M. Manka'aFri, J.E. Nguve, R.A. Ngwese, F.N. Njume, F. A. Bertha, L. Ayong, R. Njemini, L. Vanhamme, J. Souopgui, Computational design and preliminary serological analysis of a novel multi-epitope vaccine candidate against onchocerciasis and related filarial diseases, Pathogens 10 (2) (2021) 99, https://doi.org/10.3390/pathogens10020099.
[99] D.D. Laishram, P.L. Sutton, N. Nanda, V.L. Sharma, R.C. Sobti, J.M. Carlton, H. Joshi, The complexities of malaria disease manifestations with a focus on asymptomatic malaria, Malar. J. 11 (2012) 29.
[100] H. Tripathi, P. Bhalerao, S. Singh, H. Arya, B.S. Alotaibi, S. Rashid, M.R. Hasan, T.K. Bhatt, Malaria therapeutics: are we close enough? Parasites Vectors 16 (1) (2023) 130, https://doi.org/10.1186/s13071-023-05755-8.
[101] P.S. Atchade, C. Doderer-Lang, N. Chabi, S. Perrotey, T. Abdelrahman, C.D. Akpovi, L. Anani, A. Bigot, A. Sanni, E. Candolfi, Is a *Plasmodium* lactate dehydrogenase (pLDH) enzyme-linked immunosorbent (ELISA)-based assay a valid tool for detecting risky malaria blood donations in Africa? Malar. J. 12 (2013) 279, https://doi.org/10.1186/1475-2875-12-279.
[102] Centre for Disease Control, How vaccines are developed and approved for use, How New Vaccines Are Developed (2021). https://www.cdc.gov/vaccines/basics/test-approve.html. (Accessed 21 July 2023).
[103] H.D. Chapman, B. Roberts, M.W. Shirley, R.B. Williams, Guidelines for evaluating the efficacy and safety of live anticoccidial vaccines, and obtaining approval for their use in chickens and turkeys, Avian Pathol.: journal of the W.V.P.A 34 (4) (2005) 279–290, https://doi.org/10.1080/03079450500178378.
[104] T. Kurata, Minimum Requirements for Biological Products, National Institute of Infectious Diseases, Tokyo, Japan, 2006.
[105] G.N. Singh, Diphtheria and tetanus and whole cell pertussis vaccine (Adsorbed), Indian Pharmacopoeia 3 (3) (2007) 744–757.
[106] E.P. Zorrilla, S. Iwasaki, J.A. Moss, J. Chang, J. Otsuji, K. Inoue, M.M. Meijler, K.D. Janda, Vaccination against weight gain, Proc. Natl. Acad. Sci. U.S.A. 103 (35) (2006) 13226–13231, https://doi.org/10.1073/pnas.0605376103.
[107] A.N. Oli, U.C. Oli, O.S. Ejiofor, C.U. Nwoye, C.O. Esimone, An assessment, in mice, of the safety of the childhood immunization vaccines sourced from three south-eastern states of Nigeria, Trials in Vaccinology 5 (2015) 8–14, https://doi.org/10.1016/j.trivac.2015.10.001.
[108] O.A. Nnamdi, A.R. Uchenna, O.U. Chinedum, N.C. Ugochukwu, E.O. Shedrack, E.C. Okechukwu, Safety evaluation in mice of the childhood immunization vaccines from two south-eastern states of Nigeria, Asian Pac. J. Trop. Biomed. 5 (2) (2015) 132–137, https://doi.org/10.1016/S2221-1691(15)30157-X.
[109] A. Kalra, J.R. Edula, P.K. Gupta, A.K. Pandey, V.S. Chauhan, Antigenicity of a bacterially expressed triple chimeric antigen of *Plasmodium* falciparum AARP, MSP-311 and MSP-119: PfAMSP-Fu35, PLoS One 11 (10) (2016) e0165720, https://doi.org/10.1371/journal.pone.0165720.
[110] J.S. Eacret, D.M. Gonzales, R.G. Franks, J.M. Burns Jr., Immunization with merozoite surface protein 2 fused to a *Plasmodium*-specific carrier protein elicits strain-specific and strain-transcending, opsonizing antibody, Sci. Rep. 9 (1) (2019) 9022, https://doi.org/10.1038/s41598-019-45440-4.
[111] L. Jelínková, B. Roberts, D.T. Ajayi, D.S. Peabody, B. Chackerian, The immunogenicity of a VLP-based malaria vaccine targeting CSP in pregnant and neonatal mice, Biomolecules 13 (2) (2023) 202, https://doi.org/10.3390/biom13020202.
[112] R. Weiss, W.W. Leitner, S. Scheiblhofer, D. Chen, A. Bernhaupt, S. Mostböck, J. Thalhamer, J.A. Lyon, Genetic vaccination against malaria infection by intradermal and epidermal injections of a plasmid containing the gene encoding the *Plasmodium* berghei circumsporozoite protein, Infect. Immun. 68 (10) (2000) 5914–5919, https://doi.org/10.1128/IAI.68.10.5914-5919.2000.
[113] D.A. Oyong, F.J. Duffy, M.L. Neal, Y. Du, J. Carnes, K.V. Schwedhelm, N. Hertoghs, S.H. Jun, H. Miller, J.D. Aitchison, S.C. De Rosa, E.W. Newell, M. J. McElrath, S.M. McDermott, K.D. Stuart, Distinct immune responses associated with vaccination status and protection outcomes after malaria challenge, PLoS Pathog. 19 (5) (2023 May 17) e1011051, https://doi.org/10.1371/journal.ppat.1011051.